Color Hit-or-Miss Transform on Dermatological Images

Audrey Ledoux, Noël Richard, Anne-Sophie Capelle-Laizé and Christine Fernandez-Maloigne;
University of Poitiers, XLIM-SIC JUR CNRS 7252, Poitiers, France

Abstract

The mathematical morphology is often reduced to the ordering construction and the structuring elements are limited to flat shapes. In this paper, exploiting the concept of convergence, we propose a color morphological formalism which allows bringing non-flat structuring element. Extending the mathematical morphology hit-or-miss transform to the color, we show that this formalism is adapted for complex color images, as skin images for dermatological purposes. We provide and comment results on synthetic and real images.

Introduction

The extension of Mathematical Morphology (MM) to color images is not straightforward, due to the complexity of vectorial data order. The abundance of color spaces [5] and possible color order approaches [4] lead to a quasi-infinity of expressions for color MM. Numerous authors define a total order in multivariate values [1]. However none deals with the question of color Non-Flat Structuring Element ($NFSE$) whereas they are used in some morphological operations in grayscale images (filtering [12], estimation of the fractal dimension [14] ...). In this paper we propose a new color MM in the $CIELAB$ color space that permits the definition of non-flat structuring element. We evaluate this new method using the color Hit-or-Miss Transform (HMT) to extract complex color structures in skin images.

The first part of this paper is a quick recall on the Hit-or-Miss Transform in binary and grayscale. We focus on the Barat's proposal [3]. Then, we present our color MM construction to obtain a total order allowing the definition of $NFSE$. We explain how to solve questions about a valid construction of color addition/subtraction. Next, we demonstrate the contrast selectivity of the $MOMP$ in grayscale. We evaluate this selectivity on synthetic color images. Finally, we apply and validate this approach in our applicative context of dermatology.

Table 1. *Notations*

f, $\mathscr{D}_f$	Image function and his spatial domain of definition
$\mathscr{S}_{\mathscr{D}f}$	Color coordinates domain of definition from the f function
$x = (i, j)$	Spatial coordinates for a pixel x
f^c, f^r	Complementary and reflectivity of the f function
g,$\mathscr{D}_g$	Structuring Element function and his spatial domain of definition
g', g''	Inferior and superior Structuring Element function for the $MOMP$ Transform
$h_{g'}, h_{g''}$	Value of g' and g'' function located at the spatial origin o: $g'(o) = h_{g'}$
$b'(x), b''(x)$	Minimum and maximum background value extracted on the SE border
C_x	Color coordinates of the x pixel
$\lvert\overrightarrow{C_xC_y}\rvert$	Δ_E color distance between the C_x and C_y coordinates
$O^{+\infty}$, $O^{-\infty}$	Color convergence coordinates for the dilation and the erosion
$\oplus_{\mathfrak{b}}$, $\ominus_{\mathfrak{b}}$, $\otimes_{\mathfrak{b}}$	Dilation, erosion and hit-or-miss for binary images
$\oplus_{\mathfrak{g}}$, $\ominus_{\mathfrak{g}}$	Dilation and erosion for grey-level images
$\oplus_{\mathfrak{c}}$, $\ominus_{\mathfrak{c}}$	Dilation and erosion for color images
$\underset{\mathfrak{c}}{+}$, $\underset{\mathfrak{c}}{-}$	addition and substraction for colour coordinates

Hit-or-Miss Transform

The Hit-or-Miss Transform (HMT) allows to find specific patterns in images. It was initially developed for binary images by Matheron and Serra [16]. The searched pattern is defined with a pair of disjoint Structuring Elements (SEs) that frame it, one for the foreground pattern (g') and one for the background pattern (g''). The mathematical expression of the HMT for an image f and its structuring elements $g = \{g', g''\}$ is:

$$HMT_g(I)(x) = (f \ominus g')(x) \cap (f^c \ominus g'')(x) \qquad (1)$$

where f^c is the complement of f, $f^c = \{x, x \notin f\}$.

It exists many definitions of the grayscale HMT algorithm [8, 17, 13]. In the following, we explain the Barat proposal [3], called $MOMP$ (Multiple Objects Matching using Probing). The $MOMP$ transform is an image surface probing with two SEs, one above the surface (g'') and the second below (g'). The $MOMP$ mathematical expression is a subtraction between an anti-dilation and an erosion:

$$MOMP_g(f)(x) \;=\; (f \oplus (-g'')^r)(x) - (f \ominus g')(x) \qquad (2)$$

where $g''(i, j)^r = g''(-i, -j)$.
The result value is the distance between both SEs computed at the SE origin. The pattern is found when the result is lower or equal to δ (figure 1).

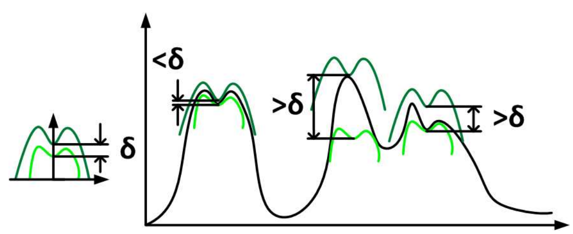

Figure 1. *Principle of the $MOMP$ transformed*

This template construction with two different SEs allows to extract a pattern with some shape and/or contrast variations and to be not very sensitive to noise in the image. To extend $MOMP$ to color, $NFSE$ have to be defined in color domain. So, the next section is de-dicated to our adapted proposal for non-flat structuring elements construction.

Color Mathematical Morphology

The most widely used methods to define minimum ($\bigvee$) and maximum ($\bigwedge$) operations in color spaces are two equivalent approaches, the *lexicographic order* or *order based on priority expressed between color axis* [11, 6]. More recently an original method was proposed by Lopez using a quaternion formalism [10].

Consequently, the dilation and erosion operators by the structuring element g, in n-dimensional space, can be expressed by (equations 3 and 4):

$$(f \oplus_{\mathbf{c}} g)(i,j) = \bigvee_{(i,j)\in\mathscr{D}_f,(k,l)\in\mathscr{D}_g} \{f(i-k,j-l)\} \quad (3)$$

$$(f \ominus_{\mathbf{c}} g)(i,j) = \bigwedge_{(i,j)\in\mathscr{D}_f,(k,l)\in\mathscr{D}_g} \{f(i+k,j+l)\} \quad (4)$$

where $\mathscr{D}_f$ and $\mathscr{D}_g$ are respectively the image support and the structuring element support.

In the majority of color *MM* construction, expressions 3 and 4 drive the color convergence toward the white and black coordinates upon the iterations. However, in color the black and the white must be only particular cases of convergence coordinates. So, in this paper, we propose a new method, called "Convergent Color Mathematical Morphology" (*CCMM*) which relies color morphological operators on this concept of *color convergence*. Two convergence coordinates are defined according to the morphological objectives. For example, the color convergence coordinates could be associated to the color set statistics [7]. Some authors have tried to construct a total ordering scheme integrating distance functions and the notion of reference colour [9]. But such approaches are not completely based on distance ordering. In addition, such approaches never define the required complementary color in terms of perception or physic property.

In the proposed method, the basic order relation between two color coordinates is built according to the distance from the convergence color points. Then the relations between two colors, C_1 and C_2, for the erosion (5) and the dilation (6) could be:

$$C_1 \preceq C_2 \quad \Leftrightarrow \quad |\overrightarrow{C_1 O^{-\infty}}| \leq |\overrightarrow{C_2 O^{-\infty}}| \quad (5)$$

$$C_1 \succeq C_2 \quad \Leftrightarrow \quad |\overrightarrow{C_1 O^{+\infty}}| \leq |\overrightarrow{C_2 O^{+\infty}}| \quad (6)$$

where $O^{-\infty}$ and $O^{+\infty}$ are respectively the convergence points of the erosion and the dilation. In equations (5) and (6), the vector norm $|.|$ uses the perceptual distance ΔE computed in *CIELAB*. In a previous work, we showed that the ΔE color distance is most accurate than other formulations or expressions in other color spaces. The (5) and (6) expressions ensure the linear convergence in a perceptual sense toward the color coordinates chosen. But they don't construct a total order as required. The complete description and the validation of a total order are not the subject of this paper, so they won't be detailed here. The definition of the maximum color coordinates on the image support $\mathscr{D}_f$ and the structuring element support $\mathscr{D}_g$, for the dilation is:

$$\bigvee_{x\in(\mathscr{D}_f\cap\mathscr{D}_g)} \{f(x)\} = \left\{C_y, C_y = \bigvee_{\forall C_x \in \mathscr{S}_{\mathscr{D}9}} \left\{C_x^{\beta}\right\}\right\} \quad (7)$$

$$\text{with} \quad \mathscr{S}_{\mathscr{D}9} = \left\{C_y : C_y = \bigvee_{\forall C_x \in \mathscr{S}_{\mathscr{D}8}} \left\{C_x^{\alpha}\right\}\right\};$$

$$\mathscr{S}_{\mathscr{D}8} = \left\{C_y : |\overrightarrow{C_y O^{-\infty}}| = \bigvee_{\forall C_x \in \mathscr{S}_{\mathscr{D}7}} \left\{|\overrightarrow{C_x O^{-\infty}}|\right\}\right\};$$

$$\mathscr{S}_{\mathscr{D}7} = \left\{C_y : |\overrightarrow{C_y C_i}| = \bigvee_{\forall C_x \in \mathscr{S}_{\mathscr{D}6}} \left\{|\overrightarrow{C_x C_i}|\right\}\right\};$$

$$\text{and} \quad \mathscr{S}_{\mathscr{D}6} = \left\{C_y : |\overrightarrow{C_y O^{+\infty}}| = \bigwedge_{\forall x \in (\mathscr{D}_f\cap\mathscr{D}_g)} \left\{|\overrightarrow{C_x O^{+\infty}}|\right\}\right\}$$

Non-flat structuring element

Using a non-flat structuring element g provides tool to weight the influence of neighbors in morphological operations. In color space, the expression of dilation and erosion are classically expressed by:

$$(f \oplus_{\mathbf{c}} g)(i,j) = \bigvee_{(i,j)\in\mathscr{D}_f,(k,l)\in\mathscr{D}_g} \{f(i-k,j-l) \underset{\mathbf{c}}{+} g(k,l)\} \quad (8)$$

$$(f \ominus_{\mathbf{c}} g)(i,j) = \bigwedge_{(i,j)\in\mathscr{D}_f,(k,l)\in\mathscr{D}_g} \{f(i+k,j+l) \underset{\mathbf{c}}{-} g(-k,-l)\} \quad (9)$$

In grayscale images, adding/subtracting to a grayscale pixel one positive scalar is taking it toward higher/lower grayscale value (toward the white/black color). With *CCMM*, we impose that color pixel displacement stills in relation with the notion of convergence. Color addition/subtraction induces the displacement of the pixels in the color space. The color vector displacement is defined by its magnitude and its orientation. Dealing with color representation, we associate the magnitude to specific color metric and we propose to use Δ_E metric. The orientation depends on the morphological operation: with addition the displacement is oriented toward convergence color coordinates. On the contrary, with subtraction, the displacement is oriented toward divergence coordinates. The figure 2 shows an example of color displacements in addition case.

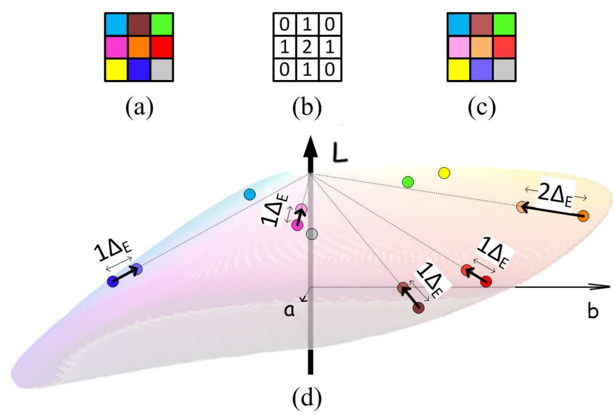

Figure 2. *Example of vector displacements with color addition, the convergence color is the white; (a) Set of colors; (b) Non-flat structuring element; (c) New set of colors; (d) Calculation of new coordinates of the set of colors.*

Selectivity of Color *MOMP* (*CMOMP*)

The *MOMP* allows to find specific objects by matching a template with a pattern chosen from application constraints. With color images, we have to notice that the term "pattern" has a particular significance: it characterizes the shape or the pixels organization in image grid (spatial organization) on the one hand and on the other hand the color organization of pixels (organization in color space). In this paper, we focus on the color selectivity.

Firstly, we define the relationship between the extracted pattern contrast[1] and the *SEs* magnitude for the grayscale *MOMP* transform. Barat [3] defines two constraints for the *MOMP* transform. The first one defines that the intersection between the two

[1] The contrast is the distance between the object and the background color.

SEs must be null, and the second one that the g'' *SE* must be above g'. For this work, we add two additional constraints, first one defining that the two *SEs* have the same spatial support $\mathscr{D}_g$, and second one on the shape that is reduced to convex hull. Given the *MOMP* algorithm, the pattern of interest is bounded by a template constructed with g' and g''. The value of g'' and g' *SEs* at their origin are respectively $h_{g''}$, $h_{g'}$. The distance between the two *SEs* is defined at the *SEs* origin by $\delta = h_{g''} - h_{g'}$. Figure 3-(b) and 3-(c) illustrate two cases where the patterns are searched in the black curve. As we focus on the contrast selectivity, all objects of our example have the same spatial organisation. Only the pattern contrast changes. Figure 3-(a) describes the used template shapes g' and g'' which have the same spatial organisation than patterns.

The image function f is defined as the sum of a $b(x)$ background function and a set of N patterns $M(x)$ (eq. 10). Each pattern $M(x)$ is defined on a spatial domain $\mathscr{D}_M$ as $M(x) = 0, \forall x \not\subset \mathscr{D}_M$ and located at the y_i location corresponding to the $\mathscr{D}_M$ origin. To be match by the *MOMP* transform the spatial domain of the f function must be $\mathscr{D}_M = \mathscr{D}_{g'} = \mathscr{D}_{g''}$.

$$f(x) = b(x) + \bigcup_{i=1}^{N} M(x - y_i) \tag{10}$$

As the patterns and the *SEs* have same spatial organisation, we study the *MOMP* transform result at the y_i location centered on the patterns to extract (figure 3-(b) and 3-(c)). With all the previous constraints, this position is the only one where the subtraction between the anti-dilation and the erosion can be smaller than δ. In the following we compute the anti-dilation and erosion at the position y_i to estimate the relationship between the extracted patterns contrast and the *SEs* magnitude.

The first part of the *MOMP* transform is the anti-dilation expression $(f \oplus_{\mathfrak{g}} -(g'')^r)$. As g'' is a symmetric convex hull, centered at the *SE* spatial origin : $(g'')^r = g''$. At y_i the pattern center position, the dilation result could be:

$$(f \oplus_{\mathfrak{g}} -(g'')^r)(y_i) = \begin{cases} f(y_i) - h_{g''} & \text{when} \quad f(y_i) - h_{g''} \geq b''(y_i) \\ b''(y_i) & \text{even} \end{cases} \tag{11}$$

In this expression, $b''(y_i)$ is the $b(x)$ background maximum value extracted when g'' is centered on the pattern (y_i coordinate) and $f(y_i)$ is the image value at this location.

The second part of the *MOMP* transform is the erosion expression $(f \ominus_{\mathfrak{g}} g')$. At the pattern center position y_i, the erosion result could be:

$$(f \ominus_{\mathfrak{g}} g')(y_i) = \begin{cases} b'(y_i) & \text{when} \quad f(y_i) - h_{g'} \geq b'(y_i) \\ f(y_i) - h_{g'} & \text{even} \end{cases} \tag{12}$$

In this expression, $b'(y_i)$ is the minimum $b(x)$ background value extracted when the centered *SE* on the object center (y_i coordinate) and $f(y_i)$ is the image value at this location.

Barat defines that to be accepted a particular pattern must present a difference between the anti-dilation and the erosion at the shape center position y_i inferior to δ:

$$((f \oplus_{\mathfrak{g}} -(g'')^r) - (f \ominus_{\mathfrak{g}} g'))(y_i) < \delta \tag{13}$$

We are interested by the definition of the minimal and maximal contrasts accepted by the *MOMP* transform to define the $h_{g''}$ and $h_{g'}$ value. Then, for the smallest contrasts, we can express that:

$$\begin{cases} (f \oplus_{\mathfrak{g}} -(g'')^r)(y_i) & = & f(y_i) - h_{g''} \\ (f \ominus_{\mathfrak{g}} g')(y_i) & = & b'(y_i) \end{cases} \tag{14}$$

$$\Rightarrow f(y_i) - h_{g''} - b'(y_i) < \delta \tag{15}$$

$$\Rightarrow f(y_i) - b'(y_i) < \delta + h_{g''} \tag{16}$$

In a similar way, for the highest contrasts we have:

$$\begin{cases} (f \oplus_{\mathfrak{g}} -(g'')^r)(y_i) & = & b''(y_i) \\ (f \ominus_{\mathfrak{g}} g')(y_i) & = & f(y_i) - h_{g'} \end{cases} \tag{17}$$

$$\Rightarrow b''(y_i) - (f(y_i) - h_{g'}) < \delta \tag{18}$$

$$\Rightarrow f(y_i) - b''(y_i) > h_{g'} - \delta \tag{19}$$

In a first approximation, we consider that $b'(y_i) = b''(y_i)$, that is the background average around the object. So if we define h_{min} and h_{max}, the minimum and maximum contrast values between the background and the shape extremum from equations (16) and (19) we have:

$$\begin{cases} h_{min} = h_{g'} - \delta \\ h_{max} = h_{g''} + \delta \end{cases} \quad \text{with } \delta = h_{g''} - h_{g'} \tag{20}$$

We directly obtain, the features to manage the *SE* magnitude:

$$\begin{cases} h_{g'} = & \frac{2h_{min} + h_{max}}{3} \\ h_{g''} = & \frac{h_{min} + 2h_{max}}{3} \end{cases} \tag{21}$$

So the *MOMP* transform can find shape contrasts which are in the range $[h_{min}, h_{max}]$, and we can note that the interval size is 3δ, so δ is the contrast selectivity unit for the *MOMP* transform.

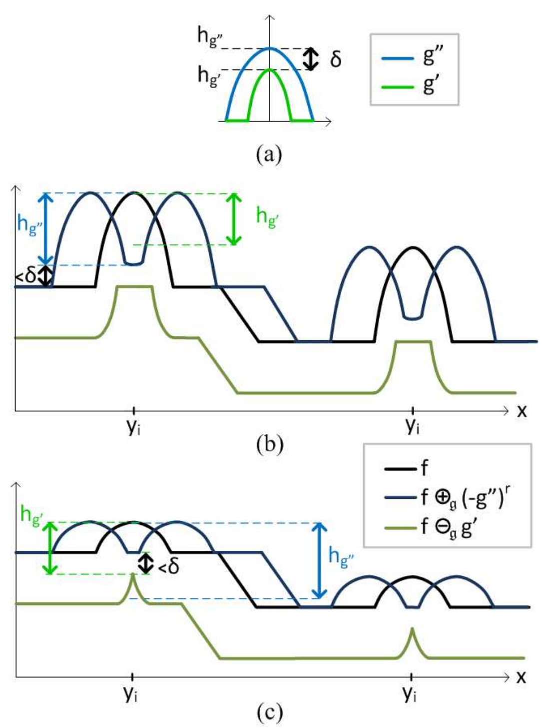

Figure 3. *(a) Structuring elements; (b) computation of anti-dilation and erosion for a f function with great contrasts; (c) computation of anti-dilation and erosion for a f function with small contrasts.*

The contrast selectivity can be easily extend to color $MOMP$. With the duality property, the totaly vectorial ordering and the definition of $NFSE$, our $CCMM$ construction allows the natural extension from gray-scale contrast selectivity to color selectivity. In the color images, the extracted patterns are selected depending on their spatial organisation and their color contrast. The $MOMP$ Transform is applied using adapted convergence color: the convergence point of the erosion ($O^{-\infty}$) is the background color and that of the dilation ($O^{+\infty}$) is the color of searched patterns. The $h_{g''}$ and $h_{g'}$ values are defined automatically and depending on the $[h_{min}, h_{max}]$ interval. This interval depends upon the color distance between both convergence points and the contrast selectivity unit δ. The searched contrast between two points is a color vector. Its direction and its norm relies on convergence points $O^{-\infty}$ and $O^{+\infty}$. A color is accepted if the contrast vector between the background and this color is exactly $\overrightarrow{O^{-\infty}O^{+\infty}}$. Moreover the $CMOMP$ allows to enlarge the contrast selectivity. The $CMOMP$ writing creates a sphere of color selection around the wished color. The sphere radius depends upon the contrast selectivity unit δ.

The next experiment shows the ability of our algorithm to extract pattern of interest from a color image. The image is made up of patterns with different colors and shapes (figure 5-(a)). The images are constructed in the RGB space. The searched shapes are color crosses of size 5 by 5 pixels with different filling colors. The structuring elements used to extract crosses are designed with contrast equal to δ ($\delta = h_{g''} - h_{g'}$) (figure 4). As we want to select a particular color for this experiment, δ is fixed to 1. Figures 5-(b)-(c)-(d) are respectively an extraction of red crosses, green crosses and blue crosses. The attempted result is obtained. The $CMOMP$ extracts all the objects matching with the pattern of interest, with no false detection. Moreover, the selected objects have exactly the searched colors.

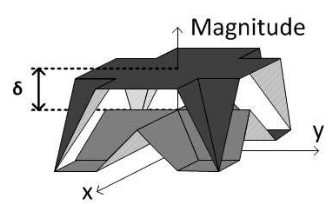

Figure 4. *3D view of the template.*

The figure 6 illustrates the impact of the color selectivity. Figures 6-(a)-(b)-(c)-(d) present an extraction of red crosses with δ parameter respectively equal to 1, 25, 40 and 55. On the figure 6-(a) only the red crosses are extracted, then on the figure 6-(b) the lighter red crosses appear, and on the figure 6-(c) the orange crosses appear. Finally, with the largest value of δ the yellow crosses appear on the figure 6-(d). In addition, we observe that the shape selectivity is well respected

This first experimental results illustrate the pattern (spatial and color) selectivity of the color $MOMP$ transform. The next section, is an application and a validation on real skin images.

Results on Skin Images
The experiment

To valid our approach construct in a perceptual point of view, we chosen to work on a dermatological images database, valuated

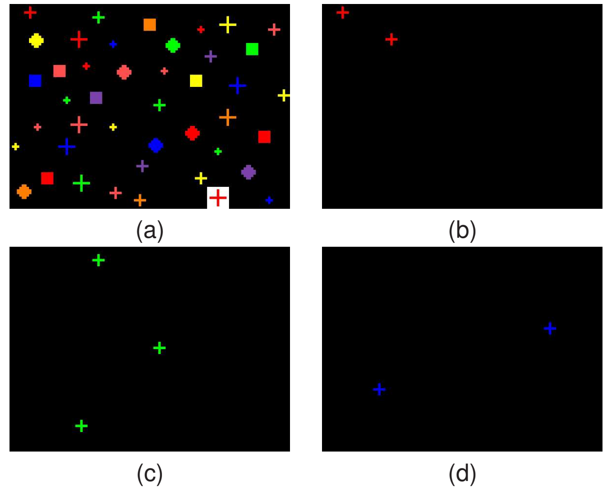

Figure 5. *(a) initial image with a black background ($O^{-\infty}$ = black); (b) detection of red crosses ($O^{+\infty}$ = red) on black background ($\delta = 1$); (c) detection of green crosses ($O^{+\infty}$ = green) on black background ($\delta = 1$); (d) detection of blue crosses ($O^{+\infty}$ = blue) on black background ($\delta = 1$).*

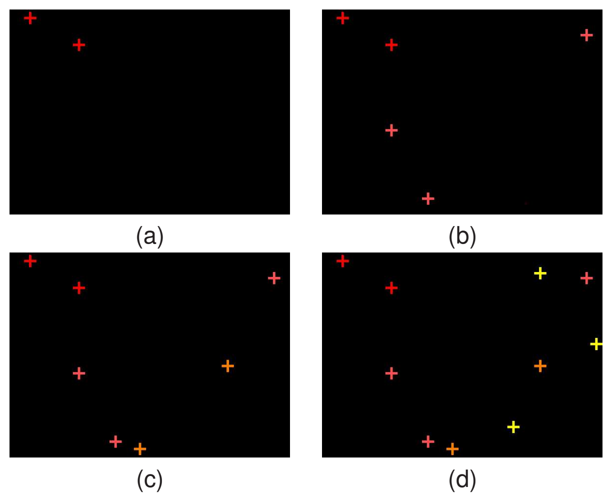

Figure 6. *Detection of red crosses (size : 5x5) on black background (a) $\delta = 1$; (b) $\delta = 25$; (c) $\delta = 40$; (d) $\delta = 55$.*

with a strict psychovisual protocol. Dermatological images are very complex color images, with a lot of diffuse color information, a lot of variations in the color background or skin artifacts or diseases depending of the human diversity of origin and life conditions. Classical ways fail to solve robust image processing routines due to this diversity, and to the fact that these images are analyzed by human expert with a non linear perception. So there's a great necessity to produce color image processing systems in accordance to the Human Visual System.

The aim of this experimental part is to find rosacea in a skin image of face. For this first evaluation, we work on some images valuated by an expert in function of rosacea level. The major difficulty of this evaluation is induced by the very low color contrast of rosacea in a skin image, in particular for the images valuated as low rank. Rosacea is defined by a sequence of connected linear segments with color close to the hemoglobin one. The more adapted shape is a line extraction. The contrast and/or the width of the rosacea is function of severity level. Then the g'' is wider and higher than the g' to allow these variations. Moreover, as the rosacea have different orientations, we apply these structuring elements in 4 directions. As the mathematical morphology does not produce spatial phase shift, the final result is the union of the results *CMOMP* with this different orientations.

Results and discussion

Some results of the *CMOMP* algorithm are shown in figures 7 to 10. The figures show the initial image (a) and the direct result of the *CMOMP* (b). For this experiment, the convergence points $O^{-\infty}$ and $O^{+\infty}$ are the color skin background and the color of the rosacea. These colors are manually chosen. We will test a statistical selection in a next study. The $[h_{min}, h_{max}]$ interval depending here also on the vector $\overrightarrow{O^{-\infty}O^{+\infty}}$. The contrast selectivity unit δ is equal to $\frac{1}{2} * |\overrightarrow{O^{-\infty}O^{+\infty}}|$.

(a) (b)

Figure 7. *(a) Image of skin with rosacea (intensity = 0); (b) color MOMP results.*

(a) (b)

Figure 8. *(a) Image of skin with rosacea (intensity = 1); (b) color MOMP results.*

As the skin and rosacea are complexe to differentiate, some false detections appear using *CMOMP*. Usually, false detections are corresponding with pores or small hair. So we delete all small patterns with a filtering to keep only the large structures. As the rosacea is a set of linear segments linked in a network, some structural criterion could be used to filter the results. So, we applied a simple post-processing filtering: all the connected pixels area (8-connexity) that contain less than 10 pixels are deleted. The figures 10-(c) show a filtering on a *CMOMP* result.

In direct *CMOMP* results or after filtering, all the searched structures are well detected, but as no reference exists for these images, it is not possible to establish an accuracy criterion. So, we propose to compare the number of pixels detected with the *CMOMP* with severity level given by expert (Table 2). In front of the severity level ranked by the experts, the amount of kept pixels by the algorithm is perfectly correlated to the expert evaluation.

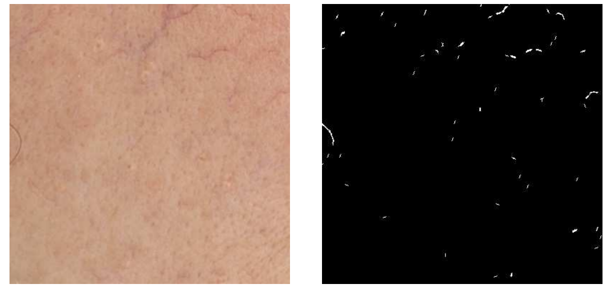

(a) (b)

Figure 9. *(a) Image of skin with rosacea (intensity = 2); (b) color MOMP results.*

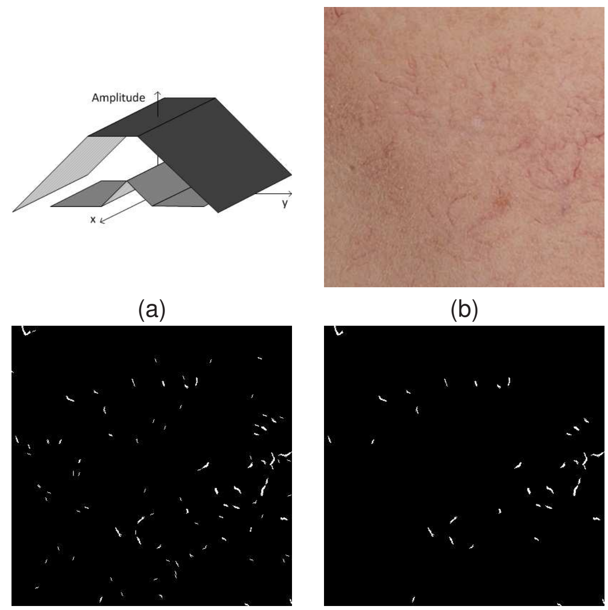

(a) (b)

(c) (d)

Figure 10. *(a) Template (b) Image of skin with rosacea (intensity = 3); (c) color MOMP results; (d) filtered result.*

Table 2. *Table of number of extracted pixels in each result images*

	CMOMP result	*CMOMP* + filtering
figure 7-(b) (severity = 0)	10	0
figure 8-(b) (severity = 1)	233	48
figure 9-(b) (severity = 2)	518	297
figure 10-(b) (severity = 3)	1073	722

Conclusion

In this paper, we present color mathematical morphology tools based on the concept of *convergence*. This new approach allows the extension of color mathematical morphology to Non-Flat Structuring Element, that had never been defined before. The originality of the expression is to solve the problem of the addition/subtraction definition in color domain. This definition uses the particular notion of the color convergence and a normalized color distance function. Consequently, the complete color mathematical morphological expression is valid in the sense of color distances standardized by the *CIE*. Thanks to this possibility, we extended the Hit-or-Miss Transform defined by Barat to the color domain. The major interest of this method is to allow template construction for color shape extraction in images. Then we show on synthetic images the capabilities of color selectivity obtained by our Color Hit-or-Miss Transform. In particular, we use a color distance function as the ΔE metric, expressed in *CIELAB*. This metric allows to extract color shapes in correlation with the Human Visual System.

The Color Hit-or-Miss Transform was applied on skin images of rosacea. The first results show that the total area of rosacea extracted by the *CMOMP* is correlated with the score given by experts. These results are very encouraging, but reliable assessment of rosacea detection algorithms is not possible on these specific images. Then we are developing a dedicated database. We are enlarging the extraction to different kinds of shapes as diffuse objects or as complex artifacts like those induced by psoriasis. But our major development lies in the extension of the *MOMP* transform in a multi-scale approach.

Acknowledgment

This work is part of project MORFISM supported by L'Oréal and ERDF (European Regional development fund).

References

[1] E. Aptoula and S. Lefèvre, "A comparative study on multivariate mathematical morphology", in *Pattern Recognition*, vol 40, 2007, pp. 2914-292

[2] C. Barat, C. Ducottet and others, "Pattern matching using morphological probing", in *Image Processing, 2003. ICIP 2003. Proceedings. 2003 International Conference on*, vol 1, IEEE, Barcelona, Spain, 2003, pp. 369-372

[3] C. Barat, C. Ducottet and others, "Pattern matching using morphological probing", in *Image Processing, 2003. ICIP 2003. Proceedings. 2003 International Conference on*, vol 1, IEEE, Barcelona, Spain, 2003, pp. 369-372

[4] V. Barnett, "The Ordering of Multivariate Data", in *Journal of the Royal Statistical Society A*, vol 139(3), 1976, pp. 318-354

[5] L. Busin and N. Vandenbroucke and L. Macaire, "volume 151 of Advances in Imaging and Electron Physics", *Chapter 2 : Color spaces and image segmentation*, Elsevier Inc., 2008, pp. 65-168

[6] A. Hanbury and J. Serra, "Mathematical morphology in the HLS colour space", in *12th British Machine Vision Conference, Manchester, UK*, Citeseer, 2001, pp. 451-460

[7] M. Ivanovici, A. Caliman, N. Richard and C. Fernandez-Maloigne, "Towards a multivariate probabilistic morphology for colour images", in *6th European Conference on Colour in Graphics, Imaging, and Vision*, 2012

[8] M. Khosravi and R.W. Shafer, "Template Matching Based on a Grayscale Hit-or-Miss Transform", in *Image Processing, IEEE Transaction on*, vol 5(6), IEEE, 1996, pp. 1060-1066

[9] J. Angulo , "Morphological colour operators in totally ordered lattices based on distances: Application to image filtering, enhancement and analysis", in *Computer Vision and Image Understanding*, vol 107(1-2), Elsevier , 2007, pp. 56-73

[10] J. Angulo, "Geometric algebra colour image representations and derived total orderings for morphological operators - Part 1: Colour quaternions", in *Journal of Visual Communication and Image Representation*, vol 21(1), 2010, pp. 33-48

[11] G. Louverdis and M.I. Vardavoulia and I. Andreadis and Ph. Tsalides, "A new approach to morphological color image processing", in *Pattern Recognition*, vol 35(8), 2002, pp. 1733-1741

[12] P. Maragos and R. Schafer "Morphological filters–Part I: Their set-theoretic analysis and relations to linear shift-invariant filters", in *Acoustics, Speech and Signal Processing, IEEE Transactions on*, vol 35(8), IEEE, 1987, pp. 1153-1169

[13] B. Naegel, N. Passat and C. Ronse, "Grey-level hit-or-miss transforms–Part I: Unified theory", in *Pattern Recognition*, vol 40(2), Elsevier, 2007, pp. 635-647

[14] S. Peleg and J. Naor and R. Hartley and D. Avnir, "Multiple resolution texture analysis and classification", in *IEEE PAMI*, vol 6, 1984, pp. 518-523

[15] B. Perret, S. Lefèvre and C. Collet, "A robust hit-or-miss transform for template matching applied to very noisy astronomical images", in *Pattern Recognition*, vol 42(11), Elsevier, 2009, pp. 2470-2480

[16] J. Serra, "Image Analysis and Mathematical Morphology", vol I, Academic Press, 1982

[17] P. Soille, "Advances in the analysis of topographic features on discrete images" in *Discrete Geometry for Computer Imagery*, Springer, 2002, pp. 271-296

Author Biography

Audrey Ledoux obtained his master's Degrees in signal processing from the University of Poitiers in 2010. Since, she is studying his PhD at XLIM-SIC (Signals, Images and Communications) JUR CNRS 7252 laboratory. His doctoral work is focused on the extension of mathematical morphology operators at color based on perceptual color distances in the CIELAB space.

Noël Richard received the M.Sc and Ph.D. Degrees from the University of Poitiers in 1988 and 1993 respectively. Since 1992, he is researcher at XLIM-SIC. His research interests include image analysis by means of fractal geometry, color and texture features. Since 2000, his work focuses on the color perception of images and texture in human vision and the link between images and semantics through ontology.

Anne-Sophie Capelle-Laizé received her PhD in Image Processing from Poitiers University, France (2003). Since 2006, she is associated Professor at the University of Poitiers, France. Her work focuses on color image processing, segmentation, data fusion and imprecise data fusion.

Christine Fernandez Maloigne is professor of signal and image processing. She manages the Department SIC of Xlim since 2008. Her actual scientific interests include image and video coding, indexing, watermarking and image quality assessment. She represents France in the Division 8 (Image Technology) of CIE and manages the TC8-12 about video and image compression assessment. She is also member of the French National Body for the ISO JPEG, since 2000.